Article

Journal of
Nanoscience and Nanotechnology
Vol. 18, 2210–2219, 2018
www.aspbs.com/jnn

Soluble and Nanoporous Silica Gel-Entrapped *C. freundii* Methionine γ-Lyase

Elena A. Morozova[1], Vitalia V. Kulikova[1], Serena Faggiano[2], Samanta Raboni[2,3], Edi Gabellieri[3], Patrizia Cioni[3], Natalia V. Anufrieva[1], Svetlana V. Revtovich[1], Tatyana Demidkina[1,*], and Andrea Mozzarelli[2,3,4,*]

[1] *Engelhardt Institute of Molecular Biology, Russian Academy of Sciences, Moscow, 119991, Russia*
[2] *Department of Food and Drug, University of Parma, Parma, 43124, Italy*
[3] *Institute of Biophysics, National Research Council, Pisa, 56124, Italy*
[4] *National Institute of Biostructures and Biosystems, Rome, 00136, Italy*

Methionine γ-lyase is a pyridoxal 5′-phosphate dependent tetramer that catalyzes the α,γ-elimination of methionine in ammonia, methanethiol and α-ketobutyrate. MGL catalytic power has been exploited as a therapeutic strategy to reduce the viability of cancer cells or bacteria. In order to obtain a stable enzyme to be delivered at the site of action, MGL can be encapsulated in a variety of matrices. As a reference encapsulation strategy we have prepared MGL nanoporous wet silica gels. Immobilized MGL gels were characterized with regards to activity, stability, absorption, circular dichroism and fluorescence properties and compared with soluble MGL. We found that MGL gels exhibit (i) spectroscopic properties very similar to MGL in solution, (ii) a higher stability with respect to the soluble enzyme and (iii) catalytic activity six-fold lower than in solution. These findings prove that MGL encapsulation is a suitable strategy for therapeutic applications.

Keywords: Methionine, Protein Drug, Protein Encapsulation, Pyridoxal Phosphate, Enzyme Activity, Fluorescence.

1. INTRODUCTION

Methionine γ-lyase (MGL) (EC 4.4.1.11) is a homotetrameric PLP-dependent enzyme that catalyzes the α,γ-elimination of methionine in ammonia, methanethiol and α-ketobutyrate. In addition, MGL catalyzes the γ-replacement of L-methionine and its derivatives. As a secondary reaction, MGL catalyzes the α,β-elimination of cysteine and S-substituted cysteines and the β-replacement reaction of these amino acids.[1,2] MGL has been isolated in bacteria and protozoa. The PLP coenzyme is bound as a Schiff base to the active site lysine residue forming the internal aldimine (Scheme 1). In the presence of the substrate methionine or other substrate analogues, MGL forms the external aldimine that in a multi-step process is converted to products. *Citrobacter freundii* MGL internal aldimine, in which PLP is bound to Lys210, exhibits an absorption band at ∼420 nm, attributed to the ketoenamine tautomer of the Schiff base, and a weak band at ∼330 nm, attributed to the enolimine tautomer of the Schiff base.[3] MGL external aldimines with some competitive inhibitors absorb at ∼430 nm whereas quinonoid intermediates formed along the catalytic processes catalyzed by PLP-dependent enzymes absorb at ∼500 nm.[4] The three-dimensional structures of MGL from *Citrobacter freundii*[5] as well as from other bacteria, including *Clostridium sporogenes* (PDB code 5DX5) and *Pseudomonas putida* (PDB code 2O7C), and from protozoa such as *Trichomonas vaginalis* and *Entamoeba histolytica* have been solved. MGL belongs to the fold type I of the PLP-enzyme structural family. Its polypeptide chain with molecular mass of around 43 kDa is composed of two domains, a small domain and a large domain, with PLP located between the two domains within the enzyme active site. MGL is a dimer of dimer with each active site containing residues of the interacting subunit. Tyr113 in the active site is highly conserved through MGLs from several species.[6–8] Cys115 replacement changes the substrate

*Authors to whom correspondence should be addressed.

 1533-4880/2018/18/2210/010 doi:10.1166/jnn.2018.14333

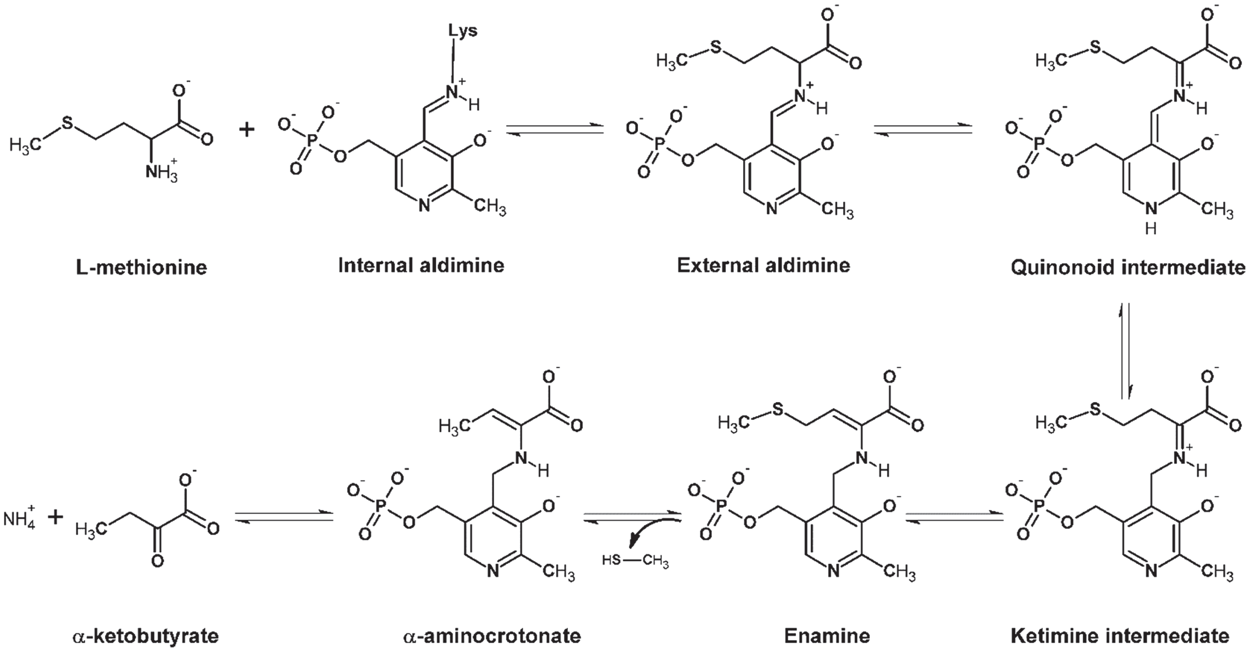

Scheme 1. Catalytic mechanism of MGL α,γ-elimination reaction.

selectivity, as demonstrated in *P. putida*,[8] *T. vaginalis*,[9] *C. freundii*,[10] and *Clostridium sporogenes*[11] MGLs.

MGL catalytic power has been exploited towards the development of drugs to reduce the viability of either cancer cells or bacteria.[12] Regarding the application in cancer, the rationale is that tumor cells require an abundant supply of methionine for proliferation.[13,14] MGL delivered in the proximity of cancer cells can lead to selective methionine degradation, thus to methionine starvation, a condition that can also be partially obtained by a rigid diet with methionine-depleted proteins.[15,16] A similar approach is applied for drugs against acute lymphoblastic leukemia, which contain *E. coli* L-asparaginase, able to deprive leukemic cells of circulating asparagine.[17] MGL can be also exploited against bacteria, since it catalyzes the degradation of substrate analogs, such as alliin and S-substituted L-cysteine sulfoxides to form allicin or S-alkylthiosulfinates, that have been demonstrated to be potent antibacterial agents. The concomitant delivery of MGL and substrate analogs to the site of infection might represent a novel antibiotic strategy.[18] For biopharmaceutical applications against either cancer or bacterial infections, MGL needs to be properly formulated in order to be protected from protease action and to increase stability, thus increasing bioavailability. Towards this goal, protein encapsulation represents a powerful strategy.[19–21] Proteins are encapsulated in micro- or nanoparticles formed by a variety of different polymeric matrices, such as polylactic (PLA) and poly(lactic-co-glycolic) acid (PLGA), alginates or chitosan.[22,23] Synthetic polymers, such as PLA and PLGA, require organic solvents for dissolution, with consequent risk of protein denaturation during particle formation. The main drawback of using natural matrices like alginate and chitosan is the possible leakage of entrapped protein due to the fast biodegradability of these materials.

A stable protein encapsulation strategy, used for the characterization of protein function and dynamics, has been achieved using organosilicate precursors of different polarities, such as tetramethylortosilicate (TMOS) or tetraethylortosilicate (TEOS). These compounds polymerize forming a silicate network that individually entraps proteins and is characterized by nanopores that allow substrate and product in and out diffusion, while immobilizing the protein within the gel matrix.[24,25] Silica nanoparticles, given their high porosity and biocompatibility, have attracted growing attention for biomedical applications.[26,27] In 2011, a silica nanoparticle drug delivery platform for targeted molecular imaging of cancer was approved by the US Food and Drug Administration.[28] A significant property of silica gels is that they are optically transparent and several spectroscopies, including UV-visible spectrophotometry, spectrofluorimetry and circular dichroism, can be used for the characterization of the entrapped proteins.[29–32] Moreover, the resulting nanoporous silica gels have been demonstrated to be a powerful tool to stabilize proteins while preserving and even enhancing their biological activities. This is achieved by selecting distinct protein conformations. For example, it was found that lipase gels exhibited about 1000 fold higher activity than the soluble enzyme because the apolar gel matrix stabilizes an open conformation of the enzyme more prone to catalysis.[33] We previously encapsulated

the PLP-dependent enzymes tryptophan synthase,[34] tyrosine phenol-lyase and tryptophan indole-lyase (TRPase),[35] obtaining enzyme gels endowed with catalytic activity, although about six-fold lower than the soluble enzyme. Interestingly, encapsulation led to a shift of the tautomeric equilibrium, stabilizing the enolimine species.

In the present work we have characterized and compared soluble and silica gel-entrapped MGL from *C. freundii* exploiting absorbance, fluorescence, circular dichroism, chemical stability and activity.

2. MATERIALS AND METHODS

2.1. Protein Preparation

MGL from *C. freundii* was expressed in *E. coli* BL21(DE3) and purified as described previously.[36] The protein was stored at −80 °C in buffer 100 mM potassium phosphate, 1 mM dithiothreitol (DTT), pH 8.0.

2.2. Encapsulation of MGL in TMOS and TEOS Silica Gels

MGL was encapsulated in silica gels following the protocols reported previously.[37–40] A solution containing tetramethyl orthosilicate (TMOS), water and hydrochloric acid was sonicated for 20 min at 4 °C. An equal volume of 10 mM potassium phosphate solution, pH 6.0, was added to the sol and the mixture was deoxygenated for 40 min at 4 °C under flux of nitrogen. The sol was mixed in 1:1 volume ratio with 5.7 mg/ml MGL solution. Encapsulation of MGL in TEOS was carried out following the protocol reported by Brennan,[40] with minor modifications. In brief, 0.33 mL of 0.1 M HCl, 0.33 mL of H_2O and 1.5 mL of TEOS were mixed in ice until a homogeneous solution was obtained. The resulting solution was stored at −20 °C. For gel preparation, 50 μL of TEOS solution were mixed with an equal volume of MGL in 100 mM potassium phosphate, pH 7.2, and layered on quartz plates (8.4 × 15.3 mm). Usually protein concentration in gel was 2.2 mg/mL. After gelification with TMOS and TEOS, quartz plates were placed in 100 mM potassium phosphate, pH 7.2, and stored at 4 °C. The absence of protein leakage from gels was checked by activity assays on the gel storage buffer. No protein was found to be released within 7 days after gel preparation.

TMOS silica gels were also prepared in the presence of PEG 1000, PEG 8000 and sorbitol, known to be potential protein stabilizers. These additives were mixed to the MGL solution prior to the addition of the sol at 0.5 and 5% w/v for PEGs and 0.25 M for sorbitol.

2.3. Enzyme Activity

MGL activity was determined using L-methionine as a substrate by measuring the rate of α-ketobutyric acid production in the coupled reaction with D-isocaproate 2-hydroxy dehydrogenase (HO-HxoDH) monitoring the decrease of NADH absorption at 340 nm ($\Delta\varepsilon = 6220\ M^{-1}cm^{-1}$) at 30 °C. The reaction mixture contained 100 mM potassium phosphate, pH 7.2, 0.1 mM pyridoxal 5′-phosphate, 5 mM DTT, 0.2 mM NADH, 70 U HO-HxoDH, and 30 mM L-methionine. Protein activity in silica gels was measured exploiting the same reaction with prior sonication of the gel matrix to avoid limitation to substrate diffusion, as described previously.[35] In brief, the micro-fragments of the gels obtained by sonication were about 4 μm, as checked with a Zeiss microscope. The fragment critical thickness over which rates are diffusion controlled can be determined using the equation:[41]

$$d_c = [(K_M + [S_0] * D'/k_{cat}[E]]^{1/2}$$

where k_{cat} and K_M are the catalytic parameters obtained in solution for *C. freundii* MGL, E is the enzyme concentration expressed in mM (0.07 mM), S_0 is the substrate concentration expressed in mM (30 mM), and D′ is the diffusion coefficient of the substrate inside the gel. D′ can be calculated from the equation:

$$D'/D = 1 - (a^2/r)$$

where a is the average molecular radius (4 Å for molecules with molecular weights in the range 200–350 daltons), D (6×10^{-6} cm²/sec) is the diffusion constant in water for substances with this range of molecular weights, and r is the average pore radius of the gel, 40–50 Å (a value of 50 Å is used). The calculated value of d_c is 150 μm, a value significantly higher than the average gel thickness of about 4 μm, indicating that diffusion of substrates within the gel fragments does not limit the reaction rates.

The absence of protein leakage after sonication of the gel was controlled by activity assays on the supernatant after centrifugation of the gel microfragments. No activity was detected, proving that sonication did not cause protein loss from the gel. The activity of MGL in solution after application of the same sonication protocol did not change. Since the addition of 5% PEG 1000 caused leakage of the protein in solution upon sonication, the activity of immobilized MGL was calculated subtracting the activity of the supernatant to that of the microgel fragments before centrifugation.

The kinetic parameters of MGL α,γ-elimination in solution and in TMOS silica gels were determined using methionine concentrations in the range between 0.05 mM and 7 mM. The enzyme concentration was 0.15 μM for soluble MGL and 1.8 μM for encapsulated MGL.

2.4. Absorbance and Fluorescence Measurements

Absorption spectra were carried out by a double beam Jasco V-550 UV/Vis spectrophotometer. Fluorescence measurements were performed using a Fluoromax-4 spectrofluorometer (Horiba Jobin Yvon, Milan, Italy). Excitation wavelength of 295 nm, 330 nm and 415 nm

were used, with an excitation and emission slit width of 5 nm. All the spectra were corrected for instrumental response. To measure fluorescence emission from encapsulated MGL, quartz plate with the protein-gel was placed in a 10×10 mm fluorescence cuvette and held with its normal at 45° from the direction of the exciting radiation. The front surface emission was collected at 90° from the excitation. Given both the measurement setup and the increase in light scattering with respect to the solution, the changes in shape of fluorescence spectrum were considered more reliable than changes in fluorescence intensity. All measurements were carried out in 100 mM potassium phosphate, pH 7.2, at 9 μM MGL (monomer concentration) in solution and 50–70 μM (monomer concentration) in gel (estimated thickness about 1 mm).

2.5. Circular Dichroism

Spectra were acquired on a Jasco J-715 spectropolarimeter in the 190–260 nm range. Spectra were recorded for a solution containing 3 μM (monomer concentration), 100 mM potassium phosphate, pH 7.2, in a quartz cuvette with optical pathway of 1 mm. A 1 mm thin film of TMOS gels containing 3 μM MGL was laid on a quartz slide and soaked in 100 mM potassium phosphate, pH 7.2, within a quartz cuvette with optical pathway of 5 mm.

2.6. MGL Stability

Chemical denaturation of both soluble and encapsulated MGL was carried out in 100 mM potassium phosphate, pH 7.2, at 25 °C, at increasing guanidinium hydrochloride (GdnHCl) concentration. Samples were incubated for 6 hours before spectroscopic measurements. Fluorescence spectra were unchanged after a further 6 hours incubation. At each denaturant concentration, the extent of spectrum shift was determined from the displacement of the center of mass of the fluorescence spectrum, ν_c,[42,43] defined as follows:

$$\nu_c = \Sigma(\lambda^{-1} \times F_\lambda)/\Sigma F_\lambda \quad (1)$$

where F_λ is the fluorescence emission at wavelength λ.

The reversibility of the unfolding reaction was assessed by measuring the degree of recovery of the center of mass of the fluorescence spectrum upon removal of denaturant. The protein, both in solution or encapsulated in TEOS and TMOS, was incubated in the presence of 6 M GdnHCl. The recovery was conducted transferring the quartz plates with encapsulated protein or diluting 30-fold the solution of denatured protein in 100 mM potassium phosphate, 0.1 mM PLP, 1 mM DTT, pH 7.2. Samples were kept at 25 °C and the refolding reaction was followed until the signal reached a constant value.

3. RESULTS AND DISCUSSION

3.1. Absorbance and Fluorescence Spectra

The absorption spectrum of MGL from *C. freundii* is characterized by the typical protein band at 280 nm, a small band at 330 nm, assigned to the enolimine tautomer of the Schiff base of PLP, and a more prominent band centered at 420 nm, assigned to the ketoenamine form of PLP (Fig. 1(A)). As a comparison the spectrum of the model PLP-valine Schiff base is reported. In the apo form bands associated to PLP absorbance disappeared as expected (Fig. 2(A)).

The fluorescence emission spectra of MGL, obtained upon excitation at 295, 330 and 415 nm, are reported in Figures 1(B–D), respectively. The fluorescence spectrum obtained by excitation at 295 nm exhibited an emission maximum centered at 333 nm (Fig. 1(B)). This emission, that originates from the single Trp residue of MGL per subunit, Trp252, suggests that this residue is located in a partially apolar environment. Indeed, the inspection of the three-dimensional structure of *C. freundii* MGL shows that Trp252 is located at the interface between monomers, in the center of the tetramer (Fig. 3(A)), surrounded by apolar residues (Fig. 3(B)). In the apo form of MGL the fluorescence intensity upon excitation at 295 nm increased significantly with respect to that of the holo form (Fig. 2(B)) indicating either a quenching of the Trp emission by the bound PLP or a conformational change that reduces non radiative emission processes. The former case seems unlikely by the absence of any emission band at higher wavelengths (see also below).

The fluorescence spectrum upon excitation at 330 nm, the wavelength where the enolimine tautomer absorbs, exhibited a band at 388 nm and a shoulder around 500 nm (Fig. 1(C)). The excitation spectrum of MGL monitored at 400 nm (data not shown) indicates that this emission originates from species absorbing at either 330 nm or 280 nm. The former species is the enolimine tautomer. The latter species might be due to either a weak energy transfer between Trp252 and PLP, a process previously observed in other PLP-dependent enzymes,[44–46] or a direct PLP absorption band centered at 290 nm. The distance between Trp252 and PLP is about 22 Å, and the planes of PLP and Trp rings are almost perpendicular (PDB 2rfv). Whereas the distance between Trp and PLP is within the possibility for an energy transfer,[47] the relative geometry of Trp and PLP well accounts for its absence. Therefore, because the absorption of PLP-valine Schiff base showed a band at 410 nm and one at 280 nm (Fig. 1(A),[48]), it is likely that the Schiff base absorbance at 280 nm is responsible of the emission at 400 nm observed for MGL. The emission at wavelengths higher than 480 nm observed upon excitation at 330 nm is likely due to an excited state proton transfer converting the enolimine to ketoenamine with emissions at 500 nm that is typical of the direct emission of the ketoenamine tautomer. This emission band was previously observed in other PLP dependent enzymes, including *O*-acetylserine sulfhydrylase[48] and tryptophan synthase.[49] When MGL was excited at 415 nm, the wavelength where

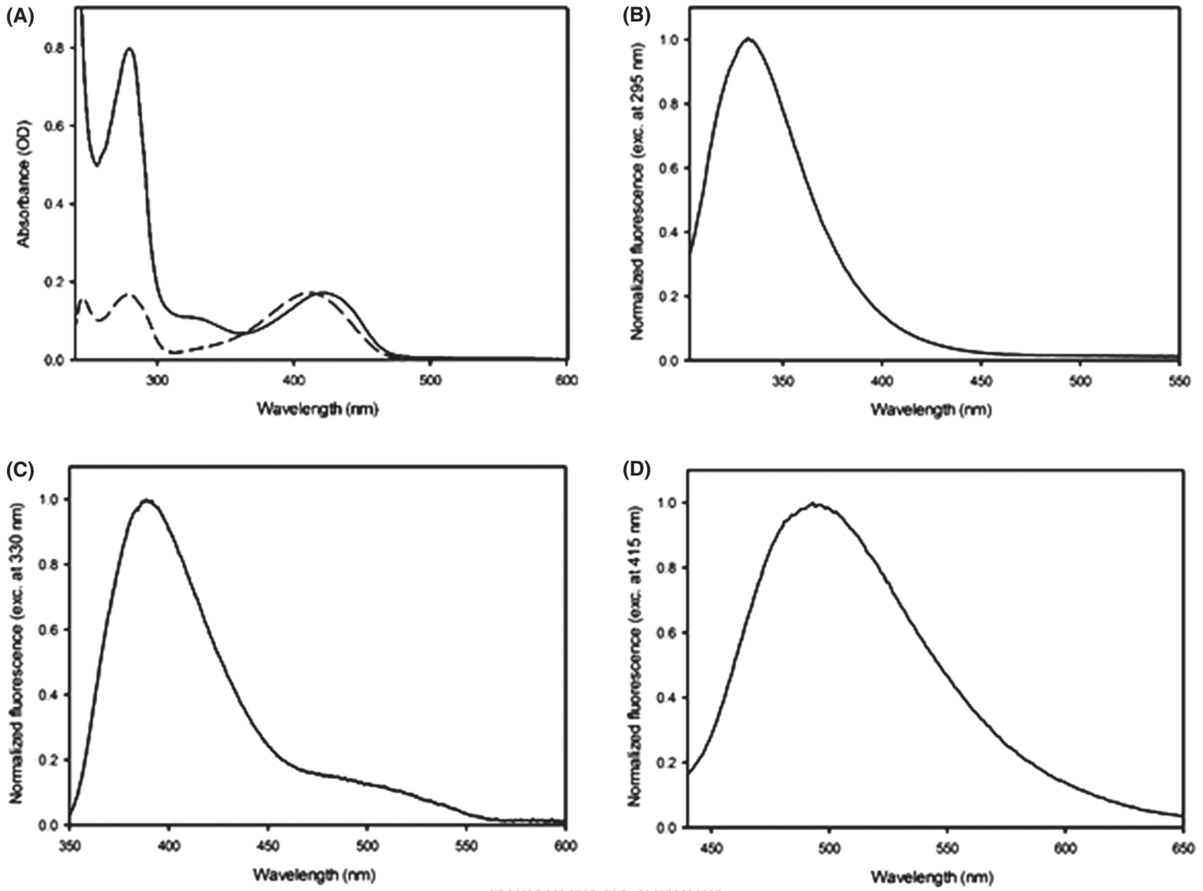

Figure 1. (A) Absorption spectrum of MGL in 100 mM potassium phosphate, 1 mM DTT, pH 8.0 (solid line), and PLP-valine (dashed line). (B–D) Fluorescence emission spectrum of MGL in 100 mM potassium phosphate, 1 mM DTT, pH 7.2, upon excitation at (B) 295 nm, (C) 330 nm and (D) 415 nm.

the ketoenamine tautomer of PLP absorbs, an intense emission band centered at 494 nm was observed (Fig. 1(D)). The excitation spectrum of MGL recorded at 500 nm indicates that the emission is originated from absorption bands at 420, 330 and 290 nm (data not shown). Thus, this confirms the excited state proton transfer of enolimine to ketoenamine as well as the involvement of a PLP band centered at about 290 nm.

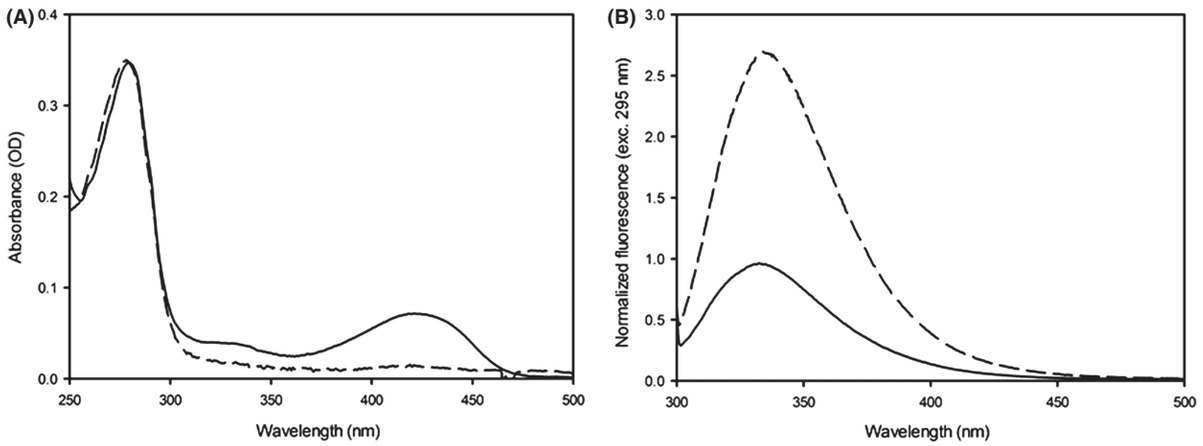

Figure 2. Comparison between the absorption spectra (A) and the fluorescence emission spectra (B) of holo- (solid line) and apo-MGL (dashed line) in 100 mM potassium phosphate, 1 mM DTT, pH 7.2. Fluorescence spectra ($\lambda_{ex} = 295$ nm) are normalized to the respective protein absorbance at 295 nm.

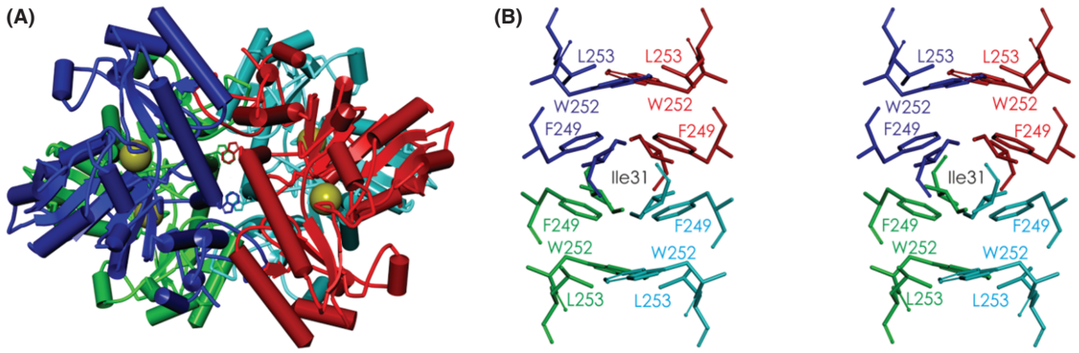

Figure 3. Crystal structure of MGL tetramer (PDB 2RFV). A. Schematic model of a tetramer. Catalytic dimers are shown in green/blue and red/cyan colors. PLP-binding sites are shown as yellow balls. Trp252 is shown as ball-and-stick representation. B. Stereoview of the hydrophobic center of tetramer.

3.2. Activity of TMOS and TEOS MGL Gels

MGL was encapsulated in silica gel as a reference entrapment method in order to evaluate the ability of the enzyme to retain its structure and activity upon immobilization. Two precursors, either TMOS or TEOS, were used to assess the potential detrimental effect of the release during gel preparation of residual amounts of methanol and ethanol, respectively, on enzyme activity and structure. It is worth noting that the resulting silicate matrix is formed by the same network of silicate bonds when the hydrolysis is complete, as it usually occurs.

MGL activity was measured on a gel micro-suspension prepared upon sonication of gels obtained from either TMOS or TEOS. MGL gels exhibited six-fold lower specific activity than in solution, indicating that encapsulation reduces the catalytic efficiency of MGL but does not abolish it. The kinetic parameters for MGL α,γ-elimination in solution and in TMOS silica gels are reported in Table I. The catalytic efficiency of the encapsulated enzyme is 6.9-fold lower compared to the soluble enzyme. A ten- to three-fold decrease in activity was also observed for tryptophan synthase,[34] tyrosine phenol-lyase and tryptophan indole-lyase[35] in nanoporous silica gels.

During the gel polymerization, the gel matrix creates a cage around the protein molecule.[50] The presence of small molecules as additives during gel formation can modulate the pore size and influence the interaction between the protein and the gel matrix.[32] The effect of osmolytes as sorbitol and of two different PEG molecules during the encapsulation process was explored in the attempt to enhance the activity of immobilized MGL.[51–53] The addition to the sol of MGL in the presence of PEG 8000 caused immediate protein precipitation at either 0.5 or 5% final PEG concentration. The activity of encapsulated MGL with 0.25 M sorbitol decreased of 10% (specific activity of 1.61 U/mg compared to 1.80 U/mg of MGL encapsulated without additives), indicating that sorbitol does not produce a significant improvement. The activity remained stable with 5% PEG 1000, but under this condition a partial loss of the protein in the solution occurred upon sonication, possibly due to the formation of larger pores. The encapsulation of MGL in the presence of 0.5% PEG 1000 produced an increase in the activity of 25%, indicating that this concentration of low MW PEG represents a beneficial additive for the encapsulation of MGL in silica gels.

Table I. Catalytic parameters of soluble and encapsulated *C. freundii* MGL.

	K_M (mM)	k_{cat} (s^{-1})	k_{cat}/K_M (mM^{-1} s^{-1})
C. freundii MGL in solution	0.81 ± 0.1	7.90 ± 0.3	9.75
C. freundii MGL in TMOS silica gel	1.30 ± 0.2	1.85 ± 0.1	1.42

3.3. Spectroscopic Properties of TMOS and TEOS MGL Gels

The absorption spectra of MGL in solution and encapsulated in silica gels from either TMOS (Fig. 4(A)) or TEOS (data not shown) are comparable. This finding suggests that the equilibrium distribution between enolimine and ketoenamine tautomers does not change in the encapsulated enzyme. The fluorescence emission bands of MGL either TMOS-derived or TEOS-derived gels are very similar to those observed in solution both for the excitation at 295 nm (Fig. 4(B)), indicating that Trp252 environment is unaltered upon gelification, and for the excitation at 415 nm (Fig. 4(D)). On the other hand, the emission band obtained upon excitation at 330 nm appeared to be shifted to shorter wavelengths than that of the soluble enzyme (Fig. 4(C)).

Circular dichroism (CD) spectra were recorded for MGL in solution (Fig. 5). The spectrum is typical of a protein containing both alpha and beta secondary structure elements. The analysis of the soluble enzyme carried out with K2D (Dichroweb) calculated a value of 52% alpha, 24% beta and 24% random, in relatively good agreement with the percentage of secondary structure elements derived

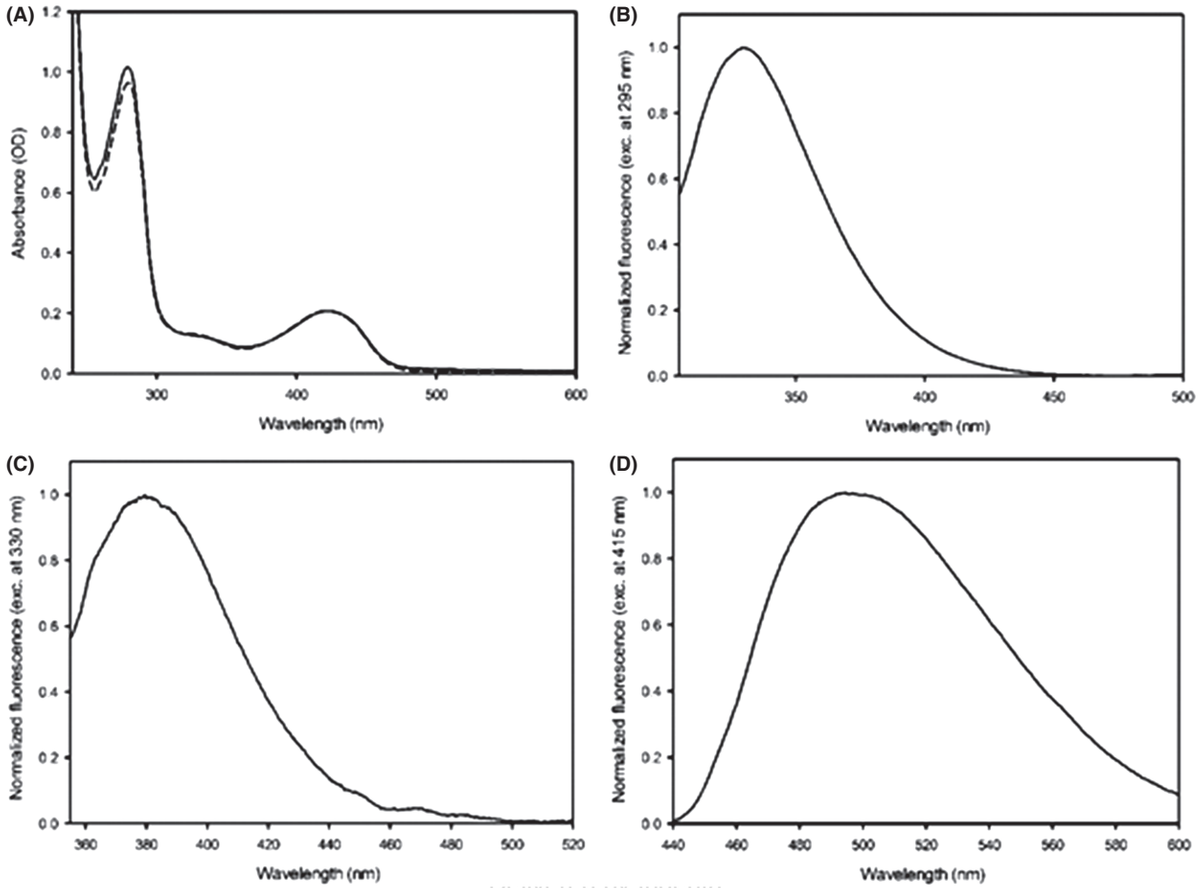

Figure 4. A. Absorption spectrum of MGL encapsulated in TMOS silica gels soaked in 100 mM potassium phosphate, pH 7.2 (solid line). The absorption spectrum of soluble MGL is shown for comparison (dashed line). B–D. Fluorescence emission spectra of MGL encapsulated in TMOS silica gels soaked in 100 mM potassium phosphate, pH 7.2, upon excitation at (B) 295 nm, (C) 330 nm and (D) 415 nm.

from the 3D structure of MGL (2RFV) that are 40% alpha, 15% beta and 45% random. Discrepancies might be due both to limitations of fitting software and small differences between solution and crystal structure. When CD spectra of TMOS MGL gels were recorded and analyzed (Fig. 5), it was found that the content of secondary structures for soluble and encapsulated MGL was the same, indicating that encapsulation in silica matrices did not alter the enzyme secondary structure.

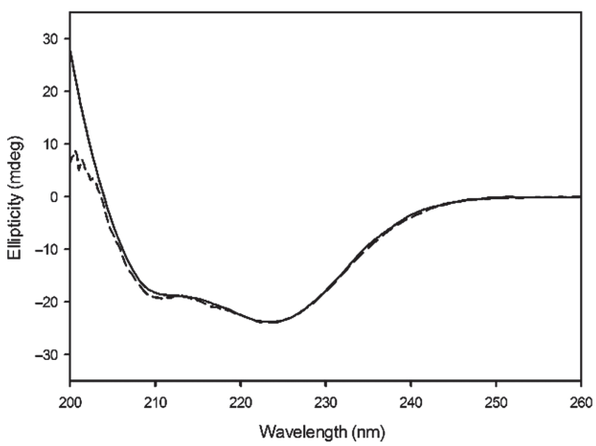

Figure 5. CD spectra of MGL in 100 mM potassium phosphate, pH 7.2 (solid line) and upon encapsulation in TMOS silica gels soaked in the same buffer (dashed line).

3.4. MGL Stability in Solution and in Silica Gels

Encapsulation of proteins in nanoporous silica gels is reported to affect stability with respect to thermal and chemical denaturation, or long-term storage.[32] The stabilizing effect of encapsulation of the protein has been previously observed,[54–57] although conflicting results have been observed.[58, 59] The stability of MGL either in solution or entrapped in TEOS silica gels was investigated monitoring absorbance (Figs. 6(A–B)) and fluorescence (Figs. 7(A–D)) changes as a function of GdnHCl concentration. Figure 6(A) shows that, for soluble MGL, the presence of 6 M GdnHCl caused the shift of the PLP absorption band from 420 nm to 390 nm, the wavelength typical of free PLP, suggesting that the coenzyme was released from the protein. For MGL encapsulated in gels (Fig. 6(B)), the addition of GdnHCl caused the

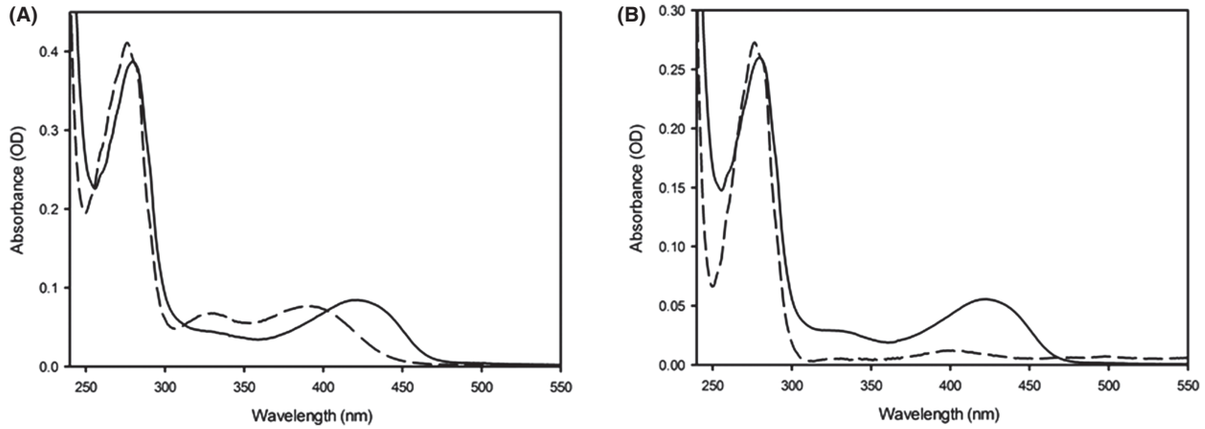

Figure 6. Denaturation of MGL in GdnHCl. Comparison between absorption spectrum of native (solid line) and unfolded in 6 M GdnHCl (dashed line) state of MGL. A. 100 mM potassium phosphate, pH 7.2 and B. TEOS-derived silica gels.

disappearance of the absorption band at 420 nm with the concomitant appearance of a weak intensity band of free PLP at 390 nm. This occurs because free PLP escapes from gel and equilibrates with the surrounding medium, that has a volume about 40-fold larger compared to the gel volume. The release of the coenzyme took place already at low concentration of denaturant for both soluble and encapsulated MGL (data not shown).

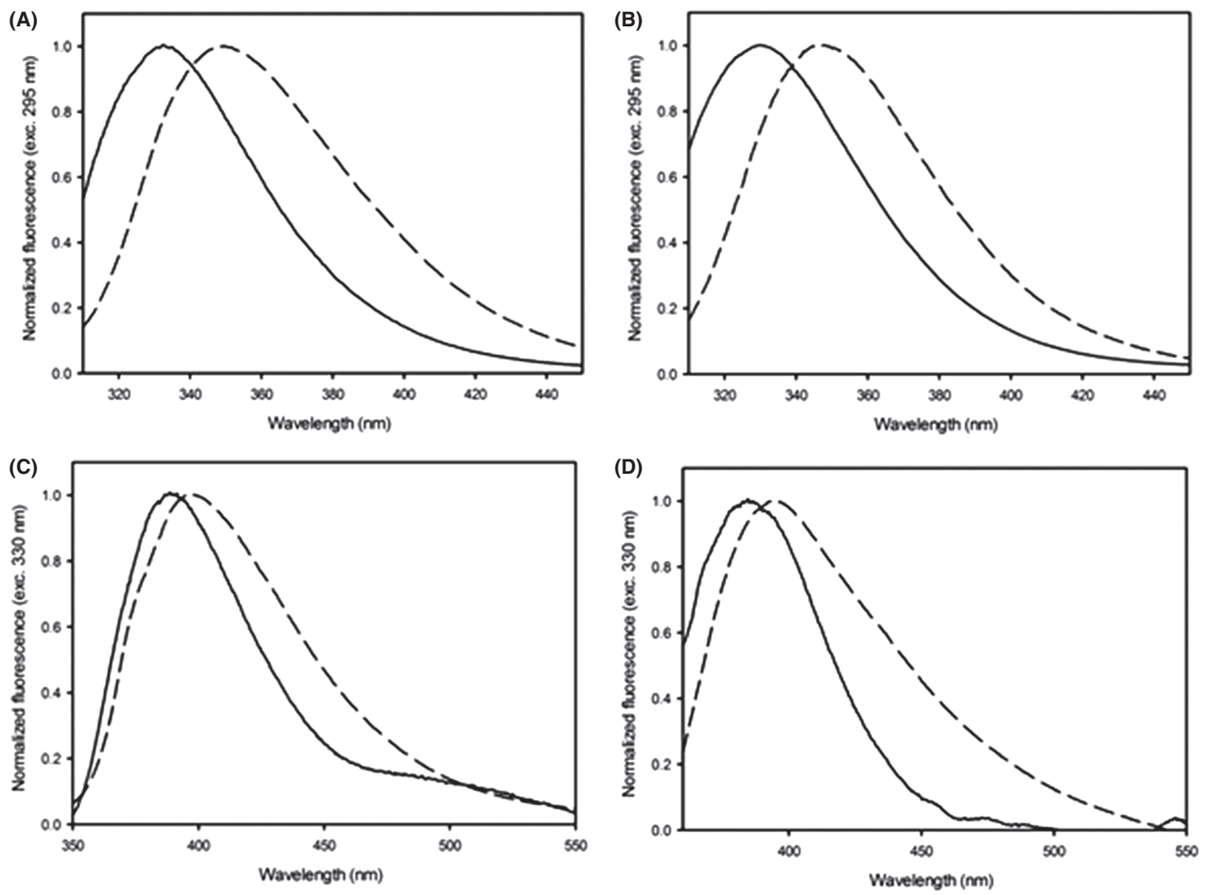

Figure 7. Changes of fluorescence emission upon denaturation. Comparison between fluorescence emission from native (solid line) and in 6 M GdnHCl (dashed line) MGL, in solution and encapsulated in TEOS gels. A and C: MGL in solution; B and D: encapsulated MGL. A and B: $\lambda ex = 295$ nm; C and D: $\lambda ex = 330$ nm.

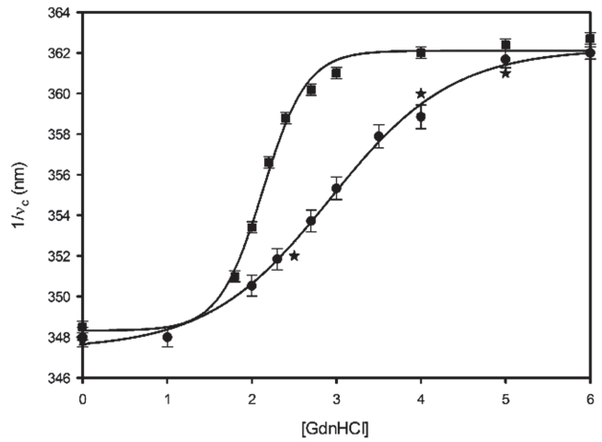

Figure 8. Equilibrium denaturation curves in 100 mM potassium phosphate, pH 7.2, at 25 °C. Samples are: Soluble MGL (squares), and MGL encapsulated in TEOS (circles) or in TMOS (stars). The line through the points represents the best fit of the experimental data to Boltzmann equation.

The spectral characteristics of the fluorescence emission of encapsulated MGL, excited at 295, 330 and 415 nm, at different concentrations of denaturant were similar to that of the protein in solution. In the presence of 6 M GdnHCl the maximum of fluorescence emission, upon excitation at 295 nm, moved from 333 nm to 350 nm (Figs. 7(A–B)), the emission wavelength typical for the unfolded form of a protein. Enzyme denaturation is accompanied by a two-fold increase in the fluorescence intensity, indicating PLP release. Upon direct excitation of the coenzyme at 330 nm, the unfolded MGL showed an increase in the emission intensity and a shift of the maximum to 396 nm (Figs. 7(C–D)), wavelength typical of free PLP. Only little changes in the shape and intensity of the fluorescence spectrum were observed upon excitation at 415 nm (data not shown).

The dependence of MGL fluorescence emission on GdnHCl concentration was determined by measuring the displacement of central of mass of protein emission, calculated as described in Materials and Methods, at increasing denaturant concentration (Fig. 8). The comparison of the denaturation curves indicates that the apparent unfolding midpoint, 2.2 ± 0.1 M in solution and 3.0 ± 0.1 M in silica gel, is shifted toward higher concentration of denaturant upon encapsulation (Fig. 8). It is likely that during encapsulation, proteins are trapped within the silica cage in pores tailored to their size and the restriction of protein mobility within this confined space results in thermodynamic stabilization of native states.[60] A straightforward analysis of the equilibrium curves obtained for MGL and the determination of meaningful thermodynamic parameters were prevented by the lack of complete recovery. Control refolding experiments for MGL in solution showed the appearance of large amount of aggregates. It is feasible that the aggregation is due to the exposure of sticky hydrophobic regions of the protein. Similar aggregation of denaturation intermediates has been observed for a wide variety of proteins.[61–63] Within the gel network, interprotein interactions are prevented and removal of denaturant after complete unfolding in 6.0 M GdnHCl results in a partial recovery of the initial fluorescence center of mass (data not shown) with no evidence of aggregation.

4. CONCLUSIONS

Our results indicate that encapsulated MGL retains most of the structural features of the soluble enzyme. The stability of MGL towards chemical denaturation increases upon immobilization. The reduction in activity is likely due to some conformational constraint during the catalytic cycle. This is also confirmed by the increase in activity measured upon addition of PEG 1000 during the polymerization process. However, the decrease in catalytic efficiency does not hamper the possibility to exploit entrapped MGL for the development of either an anti-cancer or antibiotic agent. Encapsulation of MGL in silica gels or in different matrices might represent an effective strategy to enhance the stability of the protein towards proteases in the body, to increase the bioavailability, and to reduce side effects due to protein immunogenicity.

Acknowledgments: This work was carried out with the financial support of a bilateral project between the National Research Council of Italy (CNR) (code MD P01.008) and the Russian Foundation for Basic Research (RFBR) (code 15-54-78021). Authors are grateful to Mr. Gianluca Presciuttini and Mr. Alessandro Puntoni for their valuable technical input. The Interdepartmental Center for Measurements (CIM) of the University of Parma is acknowledged for CD equipment.

References and Notes

1. H. Tanaka, N. Esaki, and K. Soda, *Enzyme Microb. Technol.* 7, 530 (**1985**).
2. H. Tanaka, N. Esaki, and K. Soda, *Biochemistry* 16, 100 (**1977**).
3. E. A. Morozova, N. P. Bazhulina, N. V. Anufrieva, D. V. Mamaeva, Y. V. Tkachev, S. A. Streltsov, V. P. Timofeev, N. G. Faleev, and T. V. Demidkina, *Biochemistry (Mosc)* 75, 1272 (**2010**).
4. L. Davis and D. Metzler, The Enzymes 3rd (edn.), edited by P.D. Boyer, Academic Press, New York (**1972**), Vol. 7, p. 33.
5. A. Nikulin, S. Revtovich, E. Morozova, N. Nevskaya, S. Nikonov, M. Garber, and T. Demidkina, *Acta Crystallogr D Biol. Crystallogr* 64, 211 (**2008**).
6. M. Fukumoto, D. Kudou, S. Murano, T. Shiba, D. Sato, T. Tamura, S. Harada, and K. Inagaki, *Biosci. Biotechnol. Biochem.* 76, 1275 (**2012**).
7. E. A. Morozova, S. V. Revtovich, N. V. Anufrieva, V. V. Kulikova, A. D. Nikulin, and T. V. Demidkina, *Acta Crystallogr D Biol. Crystallogr* 70, 3034 (**2014**).
8. D. Kudou, S. Misaki, M. Yamashita, T. Tamura, N. Esaki, and K. Inagaki, *Biosci. Biotechnol. Biochem.* 72, 1722 (**2008**).
9. A. E. McKie, T. Edlind, J. Walker, J. C. Mottram, and G. H. Coombs, *J. Biol. Chem.* 273, 5549 (**1998**).

10. E. A. Morozova, V. V. Kulikova, A. N. Rodionov, S. V. Revtovich, N. V. Anufrieva, and T. V. Demidkina, *Biochimie* 128–129, 92 (**2016**).
11. V. V. Kulikova, N. V. Anufrieva, S. V. Revtovich, A. S. Chernov, G. B. Telegin, E. A. Morozova, and T. V. Demidkina, *IUBMB Life* 68, 830 (**2016**).
12. D. Sato and T. Nozaki, *IUBMB Life* 61, 1019 (**2009**).
13. Y. Tan, M. Xu, and R. M. Hoffman, *Anticancer Res.* 30, 1041 (**2010**).
14. A. Amadasi, M. Bertoldi, R. Contestabile, S. Bettati, B. Cellini, M. L. di Salvo, C. Borri-Voltattorni, F. Bossa, and A. Mozzarelli, *Curr. Med. Chem.* 14, 1291 (**2007**).
15. P. Cavuoto and M. F. Fenech, *Cancer Treat Rev.* 38, 726 (**2012**).
16. T. Takakura, A. Takimoto, Y. Notsu, H. Yoshida, T. Ito, F. Nagatome, M. Ohno, Y. Kobayashi, T. Yoshioka, K. Inagaki, S. Yagi, R. M. Hoffman, and N. Esaki, *Cancer Research* 66, 2807 (**2006**).
17. T. Batool, E. A. Makky, M. Jalal, and M. M. Yusoff, *Applied Biochemistry and Biotechnology* 178, 900 (**2016**).
18. N. V. Anufrieva, E. A. Morozova, V. V. Kulikova, N. P. Bazhulina, I. V. Manukhov, D. I. Degtev, E. Y. Gnuchikh, A. N. Rodionov, G. B. Zavilgelsky, and T. V. Demidkina, *Acta Naturae* 7, 128 (**2015**).
19. V. R. Sinha and A. Trehan, *J. Control Release* 90, 261 (**2003**).
20. R. Solaro, F. Chiellini, and A. Battisti, *Materials* 3, 1928 (**2010**).
21. R. Vaishya, V. Khurana, S. Patel, and A. K. Mitra, *Expert Opinion on Drug Delivery* 12, 415 (**2015**).
22. S. Mohammadi-Samani and B. Taghipour, *Pharm. Dev. Technol.* 20, 385 (**2015**).
23. W. R. Gombotz and D. K. Pettit, *Bioconjug Chem.* 6, 332 (**1995**).
24. S. Bettati, B. Pioselli, B. Campanini, C. Viappiani, and A. Mozzarelli, Encyclopedia of Nanoscience and Nanotechnology, edited by H. S. Nalwa, American Scientific Publishers, Los Angeles (**2004**), Vol. 9, p. 81.
25. S. Bruno, L. Ronda, S. Abbruzzetti, C. Viappiani, S. Bettati, S. Kumar Maji, and A. Mozzarelli, Encyclopedia of Nanoscience and Nanotechnology, edited by H. S. Nalwa, American Scientific Publishers, Los Angeles (**2011**), Vol. 21, p. 481.
26. T. Andreani, A. M. Silva, and E. B. Souto, *Biotechnol. Appl. Biochem.* 62, 754 (**2015**).
27. X. Y. Li, M. Y. Wu, L. M. Pan, and J. L. Shi, *International Journal of Nanomedicine* 11, 93 (**2016**).
28. M. S. Bradbury, E. Phillips, P. H. Montero, S. M. Cheal, H. Stambuk, J. C. Durack, C. T. Sofocleous, R. J. Meester, U. Wiesner, and S. Patel, *Integr. Biol. (Camb)* 5, 74 (**2013**).
29. L. Ronda, S. Bruno, S. Faggiano, S. Bettati, and A. Mozzarelli, *Methods Enzymol.* 437, 311 (**2008**).
30. S. Abbruzzetti, S. Bruno, S. Faggiano, L. Ronda, E. Grandi, A. Mozzarelli, and C. Viappiani, *Methods Enzymol.* 437, 329 (**2008**).
31. G. Chirico, F. Cannone, S. Beretta, A. Diaspro, B. Campanini, S. Bettati, R. Ruotolo, and A. Mozzarelli, *Protein Sci.* 11, 1152 (**2002**).
32. L. Ronda, S. Bruno, B. Campanini, A. Mozzarelli, S. Abbruzzetti, C. Viappiani, A. Cupane, M. Levantino, and S. Bettati, *Current Organic Chemistry* 19, 1653 (**2015**).
33. M. T. Reetz, A. Zonta, and J. Simpelkamp, *Biotechnology and Bioengineering* 49, 527 (**1996**).
34. B. Pioselli, S. Bettati, and A. Mozzarelli, *FEBS Lett.* 579, 2197 (**2005**).
35. B. Pioselli, S. Bettati, T. V. Demidkina, L. N. Zakomirdina, R. S. Phillips, and A. Mozzarelli, *Protein Sci.* 13, 913 (**2004**).
36. I. V. Manukhov, D. V. Mamaeva, E. A. Morozova, S. M. Rastorguev, N. G. Faleev, T. V. Demidkina, and G. B. Zavilgelsky, *Biochemistry (Mosc)* 71, 361 (**2006**).
37. S. Bettati and A. Mozzarelli, *J. Biol. Chem.* 272, 32050 (**1997**).
38. S. Abbruzzetti, S. Faggiano, S. Bruno, F. Spyrakis, A. Mozzarelli, S. Dewilde, L. Moens, and C. Viappiani, *Proc. Natl. Acad. Sci. USA* 106, 18984 (**2009**).
39. L. Ronda, S. Faggiano, S. Bettati, N. Hellmann, H. Decker, T. Weidenbach, and A. Mozzarelli, *Gene* 398, 202 (**2007**).
40. J. D. Brennan, J. S. Hartman, E. I. Ilnicki, and M. Rakic, *Chemistry of Materials* 11, 1853 (**1999**).
41. S. A. Ahmed, C. C. Hyde, G. Thomas, and E. W. Miles, *Biochemistry* 26, 5492 (**1987**).
42. G. Mei, A. Di Venere, F. M. Campeggi, G. Gilardi, N. Rosato, F. De Matteis, and A. Finazzi-Agro, *Eur. J. Biochem.* 265, 619 (**1999**).
43. E. Gabellieri, E. Balestreri, A. Galli, and P. Cioni, *Biophysical Journal* 95, 771 (**2008**).
44. B. Campanini, S. Raboni, S. Vaccari, L. Zhang, P. F. Cook, T. L. Hazlett, A. Mozzarelli, and S. Bettati, *J. Biol. Chem.* 278, 37511 (**2003**).
45. G. B. Strambini, P. Cioni, A. Peracchi, and A. Mozzarelli, *Biochemistry* 31, 7535 (**1992**).
46. M. Marchetti, S. Bruno, B. Campanini, S. Bettati, A. Peracchi, and A. Mozzarelli, *Amino Acids* 47, 163 (**2015**).
47. J. R. Lakowicz, Principles of Fluorescence Spectroscopy 3rd edn., Plenum Press, New York (**2006**).
48. S. Benci, S. Vaccari, A. Mozzarelli, and P. F. Cook, *Biochimica Et Biophysica Acta-Protein Structure and Molecular Enzymology* 1429, 317 (**1999**).
49. S. Vaccari, S. Benci, A. Peracchi, and A. Mozzarelli, *Biophysical Chemistry* 61, 9 (**1996**).
50. S. Abbruzzetti, C. Viappiani, S. Bruno, S. Bettati, M. Bonaccio, and A. Mozzarelli, *J. Nanosci. Nanotechnol.* 1, 407 (**2001**).
51. J. D. Brennan, D. Benjamin, E. DiBattista, and M. D. Gulcev, *Chem. Mater.* 15, 737 (**2003**).
52. D. K. Eggers and J. S. Valentine, *J. Mol. Biol.* 314, 911 (**2001**).
53. C. M. Soares, O. A. dos Santos, H. F. de Castro, F. F. de Moraes, and G. M. Zanin, *Appl. Biochem. Biotechnol.* 113-116, 307 (**2004**).
54. D. Bolis, A. S. Politou, G. Kelly, A. Pastore, and P. A. Temussi, *Journal of Molecular Biology* 336, 203 (**2004**).
55. N. Tokuriki, M. Kinjo, S. Negi, M. Hoshino, Y. Goto, I. Urabe, and T. Yomo, *Protein Science* 13, 125 (**2004**).
56. M. Bottini, A. Di Venere, L. Tautz, A. Desideri, P. Lugli, L. Avigliano, and N. Rosato, *Journal of Sol–Gel Science and Technology* 30, 205 (**2004**).
57. K. Flora and J. D. Brennan, *Analytical Chemistry* 70, 4505 (**1998**).
58. B. Campanini, S. Bologna, F. Cannone, G. Chirico, A. Mozzarelli, and S. Bettati, *Protein Science* 14, 1125 (**2005**).
59. L. Fuentes, J. Oyola, M. Fernandez, and E. Quinones, *Biophysical Journal* 87, 1873 (**2004**).
60. D. Avnir, T. Coradin, O. Lev, and J. Livage, *Journal of Materials Chemistry* 16, 1013 (**2006**).
61. R. Rudolph, Modern Methods in Protein and Nucleic Acid Research, edited by H. Tschesche, Walter de Gruyter, Berlin (**1990**), p. 149.
62. P. Dominici, P. S. Moore, and C. B. Voltattorni, *Biochemical Journal* 295, 493 (**1993**).
63. S. Seshadri, K. A. Oberg, and V. N. Uversky, *Current Protein and Peptide Science* 10, 456 (**2009**).

Received: 13 December 2016. Accepted: 30 January 2017.